Proc. 10th New Zealand Geothermal Workshop 1988

COMPUTER SIMULATION OF A TRACER TEST AT PALINPINON-I

D. P. BULLIVANT[1], R. C. M. MALATE[2], M. J. O'SULLIVAN[1], F. X. M. STA. ANA[2]

Department of Theoretical and Applied Mechanics[1]
and Geothermal Institute[2], University of Auckland

ABSTRACT

Computer simulation is used to analyse the results of a tracer test conducted in well PN-9RD, a fluid reinjection well for Palinpinon-I (Philippines). In September 1985 a radioactive tracer I^{131} was released at PN-9RD and there were widespread and rapid returns of tracer to the production area. The computer simulator is based on a model for the fluid flow in the reservoir which can include the effects of injection wells, production wells, a single fracture and background flow. The best agreement between the transit times for the actual test and the simulation are obtained for a high permeability fracture across the field (predominantly west to east) and background flow towards the west.

INTRODUCTION

Palinpinon is a liquid-dominated geothermal reservoir located at Puhagan, Southern Negros (Philippines). A map of the area is shown in Figure 1. The behaviour of the reservoir is dominated by the presence of a number of large faults which have been investigated by several tracer tests.

After previous chemical and radioactive tracer tests had established the rapid communication between the easterly reinjection wells with the production sector, the bulk of the reinjection was shifted to the west, particularly PN-7RD, PN-8RD and PN-9RD. This move resulted in an increase in reservoir chloride and percentage reinjection returns in the westerly and

FIGURE 1. Map of the Southern Negros geothermal field

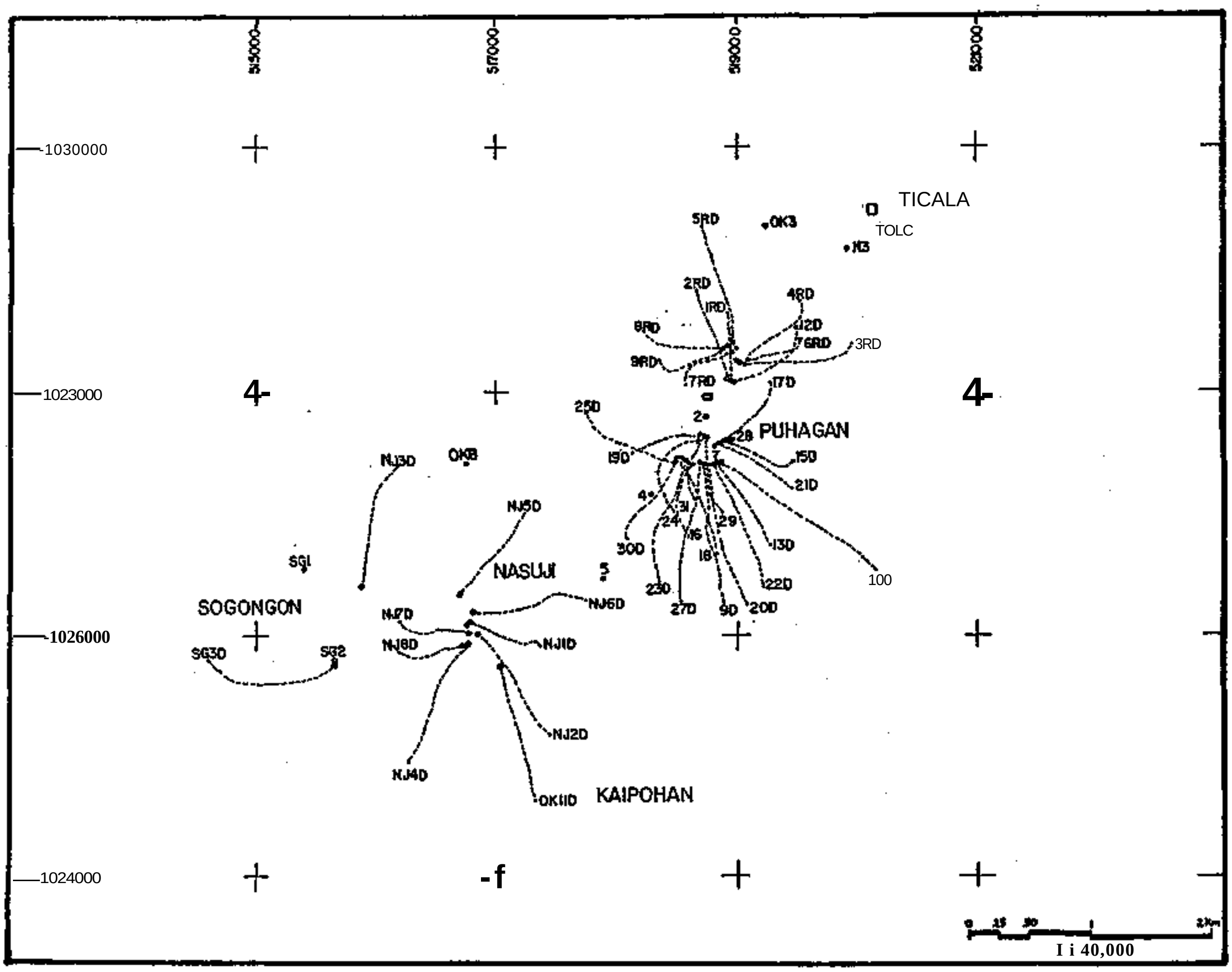

central production wells. As chloride returns could not quantitatively pin point the individual sources of the fluid returns, further tracer tests were carried out, using PN-9RD as the source reinjection well.

The objective of the test, apart from quantifying the rate and extent of communication between the reinjection well and the production area, is also to establish and correlate the tracer response with geologic structures believed to control the productivity of the Puhagan wells. A secondary objective is to assess the technique employed in conducting the test and the analysis of the results of the test, and evaluate its advantages and limitations over the other tracers.

A precursory test, using 10 kg of sodium flourescein, was conducted to obtain initial and qualitative information regarding PN-9RD reinjection fluid flow trends. This was used as the basis for preparation of the more detailed monitoring program for the subsequent test using I^{131}.

Two 5 ml glass vials containing a total of 67 Gbql (1.81 Ci) of I^{131} (half life of 8 days) were introduced into the well through a special setup connected to the wing valve of the wellhead. Sampling and monitoring of all discharging wells was carried out over a period of 24 days from 24 September 1985. Five litre samples were collected from the discharge fluid at hour intervals for 14 days and for 2 hour intervals for the following 10 days. The reinjection lines were also monitored during the test. Results of the analysis of the test are shown in Table 1.

In the past, the results of tracer tests have usually been discussed in qualitative terms only, and then often only in terms of separate connections between the tracer release well and each observation well. In the present work the complete test, that is the response of all wells to the tracer release, is analysed quantitatively.

A complete development of the simulation technique used in this paper is given in Bullivant [1988]. The flow field in the reservoir is approximated by a two dimensional, single layer, mathematical model which ignores changes in fluid velocity with depth. The model assumes that the reservoir is uniform apart from at most one straight fracture of finite length. The fracture can act as either a fast path for fluid flow or as a barrier to fluid flow (across the fracture). The fluid flow is driven by production/injection wells and natural recharge/discharge. The natural recharge/discharge appears in the model as a background flow with constant speed and direction.

From the model for the reservoir flow field, an approximation to the fluid velocity at any point in the reservoir can be calculated. The tracer particles move with the fluid particles. Thus using the fluid velocities, the path taken by a tracer particle can be numerically calculated. The destination well and the time of travel can also be calculated.

At an injection well, there is fluid leaving in all directions so that tracer can be carried to different wells along different paths. After entering a high permeability fracture, tracer can go to different production wells from different parts of the fracture.

The simulator uses the following dimensionless coordinates and parameters

$$x_d = \frac{x}{R_c}, \quad y_d = \frac{y}{R_c}$$

$$t_d = \frac{Q_c t}{\pi \phi H R_c^2}, \quad v_d = \frac{\pi \phi H R_c}{Q_c} v \qquad (1)$$

where R_c is a characteristic distance, Q_G is a characteristic flow rate, § is the reservoir porosity, H is the vertical reservoir thickness and v is the background flow speed.

SIMULATION

The average times for the I^{131} tracer to travel from the reinjection well PN-9RD to the production wells are given in Table 1. The wells are ordered by the proportion of tracer recovered ie most tracer was recovered at OK-7, less at PN-29D and so on. Table 1 is a partial reproduction of Table 2 from Urbino et al. [1986].

TABLE 1. PN-9RD tracer test results.

well	I^{131} average transit time (days)
OK-7	5.7
PN-29D	14.0
PN-26	11.0
PN-28	10.3
PN-18D	15.6
PN-30D	15.7
PN-23D	15.8
PN-31D	16.0
PN-16D	tracer found in samples after 8-19 days
PN-19D	tracer found in samples after 15-19 days
PN-17D	no response
OK-9D	no response

Well positions and production rates are required for the simulations. These are given in Table 2. Dimensionless coordinates, (1), have been used with characteristic length R_c=1000 m and characteristic flow rate Q_c=710 kgs^{*1}. The production rates have been normalized by Q_c. Because the wells are deviated, the well positions are those of the major permeable zones.

TABLE 2. Well positions and production rates.

well	x_d	y_d	Q
OK-7	0.85	1.48	0.066
PN-29D	0.77	1.39	0.073
PN-26	0.81	1.61	0.004
PN-28	1.92	1.62	0.011
PN-18D	0.74	1.02	0.046
PN-30D	0.20	1.06	0.084
PN-23D	0.31	0.88	0.083
PN-31D	0.67	1.55	0.024
PN-16D	0.48	1.15	0.053
PN-19D	0.15	1.52	0.096
PN-17D	1.20	1.90	0.032
OK-9D	0.84	0.45	0.049
PN-1RD	0.95	2.28	-0.123
PN-2RD	0.72	2.58	-0.036
PN-5RD	0.91	2.79	-0.073
PN-8RD	0.48	2.38	-0.047
PN-9RD	0.39	2.21	-0.098

For the first simulation neither a fracture nor background flow was included (the simplest model). Tracer travelled to wells PN-16D and PN-19D with the travel time to PN-16D about twice that to PN-19D. These results do not match the observed responses.

Then a high permeability fracture running down the field from near the release the well, PN-9RD, to the well which responded first and strongest, OK-7, was investigated. The investigation involved performing a number of simulations with different fracture end points. The "best-fit" simulated results, for fracture A in Figure 2, are compared with the actual results in Table 3. The dimensionless time from the simulation were converted to times in days by assuming that the dimensionless travel time to OK-7 corresponds to the actual transit time, 5.7 days.

TABLE 3. Travel times for a high permeability fracture from near PN-9RD to OK-7 (fracture end points (0.6,2.3) and (1.0,1.1))

well	dimensionless travel time	simulated travel time (days)	actual travel time (days)
OK-7	0.30	5.7	5.7
PN-29D	0.37	7.0	14.0
PN-26	no response		11.0
PN-28	no response		10.3
PN-18D	0.71	13	15.6
PN-30D	3.6	68	15.7
PN-23D	no response		15.8
PN-31D	0.56	11	16.0
PN-16D	1.3	25	8-19
PN-19D	1.4	27	15-19
PN-17D	no response		no response
OK-9D	no response		no response

The porosity-thickness product for the reservoir can be calculated using (1) as

$$\phi H = \frac{Q_c}{\pi R_c^2} \frac{5.7 \text{ days}}{0.30} = 0.37 \text{ m} \qquad (2)$$

FIGURE 2. Flow field features used for the simulations in Table 3 (A) and Table 4 (B and C).

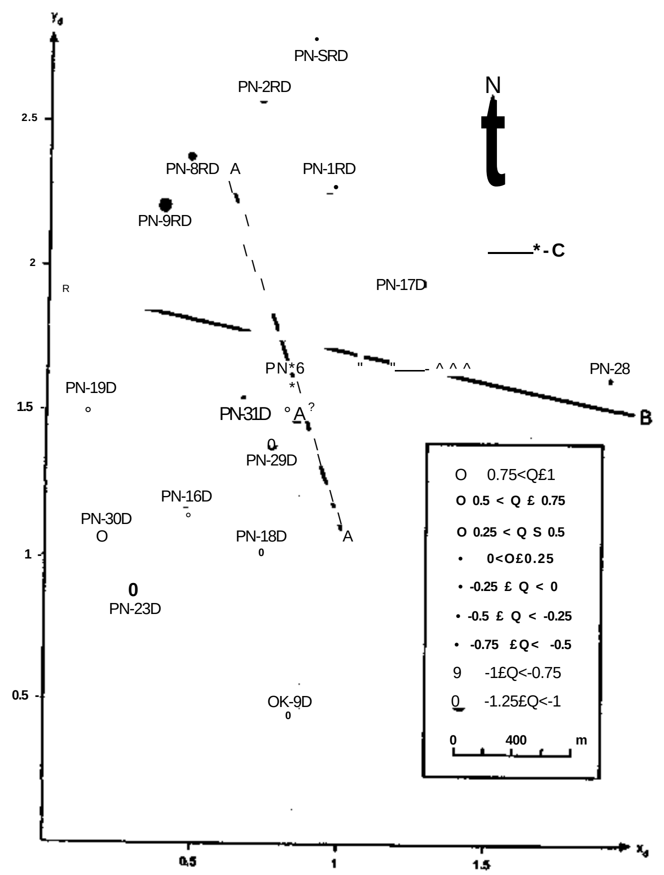

Note that Q_c has been converted from a mass flow rate to a volume flow rate using a density of 1000 kg m^{-3}. Urbino et al. [1986] calculated porosity-thickness products 1 to 2 orders of magnitude less than this, but their calculations were for individual fracture paths and not the whole reservoir.

The main defect with this simulation is that PN-26 and PN-28 do not respond. To make PN-26 respond, the fracture has to virtually intersect it (this is because PN-26 has a small production rate). Then the travel time to PN-26 is smaller than that to OK-7.

To try and make PN-28 respond a fracture across the field was investigated. Because most of the production is on the western side, there has to be background flow across the field from west to east for fluid to flow along the fracture to PN-28. The simulated travel times for the best combination of fracture (B in Figure 2) and background flow (C in Figure 2) found are compared with the actual results in Table 4. The background flow is in a direction out of the fracture so that tracer will go out to PN-28. As for Table 3, the simulated travel time to OK-7 has been made to correspond to the actual travel time.

TABLE 4. Travel times for a high permeability fracture across the field (end points (0.1,1.9) and (2.0,1.5)) with background flow (v_d=0.2 in a direction 100° clockwise from north).

well	dimensionless travel time	simulated travel time (days)	actual travel time (days)
OK-7	0.59	5.7	5.7
PN-29D	1.4	14	14.0
PN-26	no response		11.0
PN-28	0.82	7.9	10.3
PN-18D	3.8	37	15.6
PN-30D	no response		15.7
PN-23D	no response		15.8
PN-31D	0.61	5.9	16.0
PN-16D	2.0	19	8-19
PN-19D	no response		15-19
PN-17D	no response		no response
OK-9D	no response		no response

Using the dimensionless coordinates, (1), the reservoir porosity-thickness product and the background flow speed can be calculated

$$\phi H = \frac{Q_c}{\pi R_c^2} \frac{5.7 \text{ days}}{0.59} = 0.19 \text{ m} \qquad (3)$$

$$v = \frac{Q_c}{\pi \phi H R_c} v_d = 2.4 \cdot 10^{-4} \text{ ms}^{-1}$$

$$= 0.85 \text{ m/hour} = 20 \text{ m/day} \qquad (4)$$

The model giving Table 4 (fracture across the field with background flow) is better than the model giving Table 3 (fracture down the field from near PN-9RD to OK-7) because PN-28 responds. However it does not reproduce the response at PN-26. The response at PN-26 could be due to secondary fracturing, from the main fracture (B in Figure 2) towards PN-26. At present a second fracture cannot be included in the simulator, but recent work by the authors may allow consideration of a branched fault in future models. Such models may be able to match the field data better than the simple models with single fracture considered here.

CONCLUSION

Two models were each able to partially explain the test results. The first has a fracture running down the field from near PN-9RD to OK-7 (A in Figure 2). The second has a fracture across the field (B in Figure 2) with background flow of speed 20 m/day in a direction (C in Figure 2) more northerly than the fracture direction.

Analysis of the structural map of the field (Figure 3) indicates that fault A (Figure 2) computed from the computer simulation corresponds to the northerly structure (Fault "F") intersected by PN-9RD and OK-7, as reported by Urbino et al. (1986). Similarly, it is found that Fault B (Figure 2) would represent the west-east fault "X".

The results confirm that permeability and production in Puhagan are primarily controlled by structures; it indicates that there are preferred flow paths for the return of injected fluid to the production area.

Actions have been initiated to minimize, if not avoid, the detrimental effects of the reinjection on the performance of the production. Already, injection wells that have been found to contribute large amounts to returns have been given low priority in terms of utilization. Reinjection has been shifted much further away from the production bore field by utilizing wells N-3 and OK-3 (Figure 1). And, production has been concentrated on areas where minimal effect of reinjection returns are felt (southern and southwestern production wells).

REFERENCES

Bullivant, D. P. Tracer testing of geothermal reservoirs, PhD thesis, 223 pp., University of Auckland, New Zealand, 1988.

Urbino, M. E. G., M. C. Zaide, R. C. M. Malate and E. L Bueza, Structural flowpaths of reinjected fluids based on tracer tests - Palinpinon I, Philippines, Proceedings. 8th New Zealand Geothermal Workshop. 53-58, 1986.

FIGURE 3. A structural map of the Southern Negros field